Are motor proteins power strokers, Brownian motors or both?

Brian Geislinger[a], Erin Darnell[b], Kimberly Farris[c], and Ryoichi Kawai[a]

[a]Dept. of Physics, Univ. of Alabama at Birmingham, 1530 3rd Ave. S., Birmingham, AL 35294-1170;
[b]Columbia Univ., New York, NY 10027-6902;
[c]Jefferson County International Baccalaureate, Birmingham, AL 35210

ABSTRACT

About a decade ago Brownian motors were introduced as a possible mechanism for motor protein mobility. Since then many theoretical and experimental papers have been published on the topic. While some experiments support Brownian motor mechanisms, others are more consistent with traditional power stroke models. Taking into account recent experimental data and molecular level simulations, we have developed a stochastic model which incorporates both power stroke and Brownian motor mechanisms. Depending on parameter values, this motor works as a power stroker, a Brownian motor or a hybrid of the two. Using this model we investigate the motility of single-head myosins, two-head myosins and a group of myosins (muscle). The results are compared with some experimental data.

Keywords: Molecular motors, Brownian motors, thermal ratchet, motor proteins, myosin II, myosin V, actin

1. INTRODUCTION

Motor proteins such as myosin and kinesin produce directed motion against an externally applied load by consuming the chemical energy stored in ATP. The mechanism used by molecular motor proteins to convert this chemical energy directly into mechanical work has been a matter of debate for many years. After Huxley revealed that muscle contractions were a result of myosin and actin filaments sliding relative to each other,[1,2] theories were soon after developed into what is known as the lever-arm theory to explain the sliding motion.[3–6] Recently there have been a number of techniques developed capable of observing single protein-filament interactions. The resulting experiments over the past decade have led to disparate ideas about the mechanism for force generation in motor proteins. While some experiments provided data supporting Huxley's original lever-arm model, other experiments showed evidence of a Brownian motor mechanism.

Recent experiments clearly show that myosins attached to actin filaments spend most of the time in two different orientations corresponding to pre- and post-powerstroke positions.[7] X-ray crystallographic analysis of myosin protein structures have yielded evidence of multiple stable conformations of the lever arm consistent with experimental observations.[8–11] When the length of the lever arm is modified, the step length of the motor protein is also changed in a way consistent with the lever arm model.[12–18] However, contradicting experimental data were also reported by other groups.[19–24] Evidence supporting a Brownian motor mechanism can be found by examining the traveling distance of myosin for a single ATP consumption. In some experiments, myosin moves further than the lever arm is physically capable of reaching in a single powerstroke.[25] On the other hand, there have also been criticisms that Brownian motor models are not capable of producing a sufficiently strong force.[26] In this proceeding paper, we attempt to construct a single model that captures both the lever arm and Brownian motor mechanism. One becomes more dominant than the other depending on the chemical environment. With this model, we try to explain the conflicting experimental results.

The hydrolysis of ATP plays an essential role in creating the directed motion observed in motor proteins. Simultaneous observations of ATPase and mechanical motion have been made on single myosin proteins[27] that

Further author information, send correspondence to Ryoichi Kawai (E-mail: kawai@uab.edu)

Noise in Complex Systems and Stochastic Dynamics III, edited by
Laszlo B. Kish, Katja Lindenberg, Zoltán Gingl, Proc. of SPIE Vol. 5845
(SPIE, Bellingham, WA, 2005) · 0277-786X/05/$15 · doi: 10.1117/12.609464

demonstrate the tight coupling between ATP hydrolysis and the displacement/force generation of myosin. Although the actual hydrolysis cycle takes several steps,[26, 28] it is often approximated by a three-step cycle:

$$A + M \cdot ATP \underset{k_{21}}{\overset{k_{12}}{\rightleftharpoons}} A \cdot M \cdot ADP \cdot P_i \underset{k_{32}}{\overset{k_{23}}{\rightleftharpoons}} A \cdot M + ADP + P_i \underset{k_{13}}{\overset{k_{31}}{\rightleftharpoons}} A + M \cdot ATP \tag{1}$$

where A, M, P_i represent actin, myosin, and inorganic phosphate, respectively. The dot between two molecules indicates that they are bound together. The ATP hydrolysis cycle is tightly correlated to the motor's mechanical movement. When ATP is bound to the motor domain of myosin, the motor remains detached from the actin filament (unbound state). In the process of hydrolyzing the nucleotide, the myosin attaches to the filament. However, this binding is not very strong (weakly bound state). As ADP is released, the motor protein enters the rigor state, in which it is locked in its position on the filament until another ATP nucleotide is bound. At this chemical stage, the binding between the myosin and actin filament is very strong (tightly bound state). The new ATP releases the motor protein from the filament and a new cycle begins. This mechanochemical cycle is well studied and most theories are based upon it.[25–27, 29, 30] The question is how this cycle is translated into the production of mechanical work.

Based on the lever arm mechanics, releasing the inorganic phosphate, P_i from the myosin induces the "powerstroke" conformational change that swings the lever arm.[26] Since this process is too slow in the absence of the actin, we assume that the release happens when the myosin is bound to actin. With one end of the motor domain attached to the filament, the conformational change pivots the motor about that point shifting the opposite end. When the myosin is detached from actin, the lever arm swings back to the original angle, but does so about a pivot point near the neck of the motor. Due to this asymmetric cycling of the swing in the motor domain, the myosin moves in one direction. The ATP hydrolysis serves two roles in this model. One purpose is driving the conformational change in the neck region of the myosin inducing the swinging motion of the lever arm. The other purpose is to detach the myosin from the actin filament, thus changing the axis of rotation of the lever arm.

The Brownian motor mechanism utilizes the hydrolysis cycle in a quite different way. A myosin with an ATP nucleotide is free to diffuse since it is not bound to an actin filament. After hydrolyzing the ATP, the myosin moves to the nearest active site on the actin filament. While the actin filament is periodic, the spatial symmetry is broken. Therefore, myosin moves in one direction on average. Unlike the lever arm mechanics, the work is not generated by the conformational change. Instead, the myosin is actually rectifying the randomly fluctuating stochastic forces exerted by surrounding fluid molecules. The role of ATP is to switch on and off the asymmetric potential. This on-off or flashing ratchet mechanism[31–33] has drawn significant interest since it looks like a type of Maxwell's demon. While it is not possible to rectify fluctuations in thermal equilibrium due to the second law of thermodynamics, this mechanism clearly demonstrates that under certain nonequilibrium conditions thermal fluctuations can indeed be rectified.

2. THE MODEL

A key element in the lever arm mechanism is the coupling between the rotational and translational motions since the symmetric powerstroke would not otherwise produce any translational motion. Therefore, it is necessary to consider two degrees of freedom, the translational coordinate x and rotational coordinate θ defined in Fig. 1.

2.1. Two-state model

To begin with, we consider a simple two-state model. Under typical physiological conditions found in muscle,[26] the reaction rates k_{12}, k_{23}, and k_{31} are much larger than the rates k_{21}, k_{32}, and k_{13}. Furthermore, the first process is much slower than others ($k_{12} \ll k_{23}, k_{31}$). In this case, we can ignore the reverse reactions. As a further reduction, we do not have to distinguish the weakly and strongly bound states and can assume that the reaction immediately proceeds to the third state. This two-state model is useful to learn the underlying mechanism.

Like the popular on-off ratchet, the myosin alternately experiences free diffusion and a periodic potential in the translational degree of freedom. However, the rotational degree of freedom also experiences different potentials according to the conformational changes in the protein.

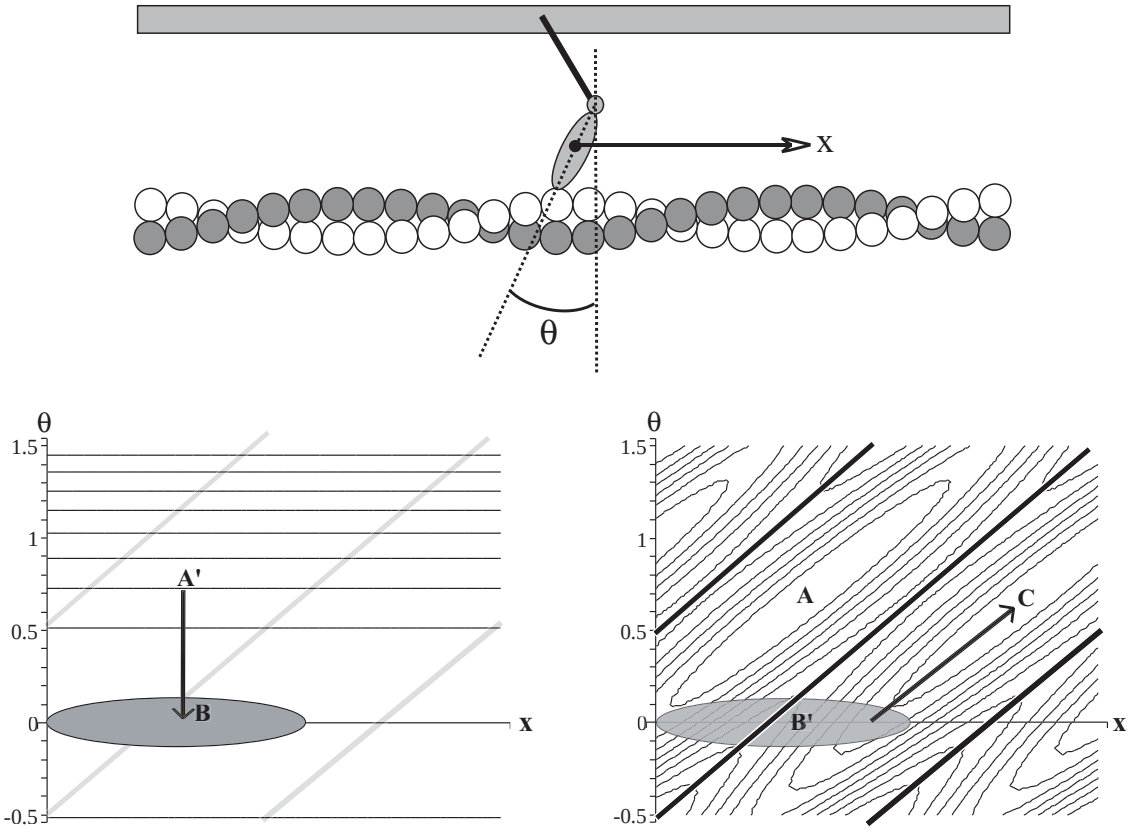

Figure 1. (*Top*) Model of myosin protein movement with two degrees of freedom. The position of the center of mass of the motor domain along the actin filament is denoted by $x(t)$. The angle that the motor domain makes with respect to a normal along the actin filament is represented by $\theta(t)$. (*Bottom, right*) Beginning in the rigor state at A the motor is rigidly held to the actin filament. (*Bottom, left*) Upon release from the filament, the motor drifts to a new equilibrium point at B, while diffusing freely along the x-axis. After returning to original potential (now at B'), the motor falls into one of two potential wells depending on which side of the potential barrier it lies — represented by the thick, dark lines — either returning to A or moving one potential period forward to C.

When the motor is free from the constraints of the actin filament (bound to ATP), it is free to diffuse in x. On the other hand, θ fluctuates around an equilibrium angle θ_1. For simplicity, we assume a simple harmonic potential for θ as a first approximation:

$$V_1(x,\theta) = \frac{K_1}{2}(\theta - \theta_1)^2 \tag{2}$$

where K_1 is a spring constant. In this state, there is no coupling between translational and rotational motion.

As the protein hydrolyzes ATP and binds to actin, it perceives the periodic nature of the filament giving rise to a periodic potential in x. Again for simplicity we assume a cosine potential. However if the motor pivots about its point of attachment, the coordinates x and θ are not entirely independent of one another, as can be ascertained from Fig. 1. When the motor is attached to the actin, a change in the angle pivots the motor about that point, causing a subsequent shift in the position of the center of the motor. The resulting bound state can be summed up as follows:

$$V_3(x,\theta) = \frac{K_3}{2}(\theta - \theta_3)^2 + U_3 \cos\left[2\pi(x - r\theta)\right] \tag{3}$$

where U_3 is the depth of the periodic potential at the rigor state. Corresponding to the conformational change in the myosin neck, the equilibrium angle θ_3 is substantially shifted from θ_1 in Eqn. (2). The value r corresponds to the length of the pivot arm to the center of mass. Although θ is not necessarily small, we use the linear approximation, $rsin(\theta) \approx r\theta$. This approximation does not change the qualitative features of the present model. We denote the effective transition rates between V_1 and V_3 as $\bar{k}_{13}$ and $\bar{k}_{31}$.

Imagine that all myosins are initially in the rigor state A in the potential V_3 (See the bottom right panel in Fig. 1). When an ATP binds to the myosin, the potential switches to V_1 (bottom left panel) and the system begins to drift towards the new equilibrium at B. At the same time, the motor thermally diffuses. When the potential switches back to V_3, a portion of the diffused myosin drift to the next equilibrium position, C. The rest return to their original equilibrium position. By alternating potentials, the myosins on average move to the right much in the same way as on-off ratchets. However, it should be noted that unlike on-off ratchets both V_1 and V_3 are spatially symmetric for any fixed angle. Nevertheless, due to the coupling between the degrees of freedom, the motor can move by rectifying the thermal fluctuation. Moreover, if θ_1 and θ_3 are sufficiently different or the length of lever arm r is sufficiently large, the motors can reach the next basin without diffusion. This transport is driven by the powerstroke of the myosin. The geometric parameters $|\theta_1 - \theta_3|$ and r, and also the time scales, the transition rates and diffusion constant determine whether the motor is a Brownian motor or a power stroker.

2.2. Three states

In the more general case where some of the reverse reactions are not negligible, we must take into account all three states with the potentials:

$$V_i = \frac{K_i}{2}(\theta - \theta_i)^2 + U_i \cos\left[2\pi(x - r\theta)\right] \qquad i \in (1,2,3). \tag{4}$$

where $U_1 = 0$, representing the myosin detached from the filament. The transition between the unbound and weakly bound states is slow since the myosin search for the active site on the actin filament. Furthermore this process is reversible since the binding is weak. Therefore, we now assume $k_{21} \neq 0$, while the other reverse processes are still assumed to be small and neglected. The conformational change $|\theta_1 - \theta_2|$ should be so small that no power stroke can take place during the transition from the unbound to the weakly bound state. However, the Brownian motor mechanism is still possible as long as the diffusion is sufficiently large. During the transition from the weakly to strongly bound state, a large conformational change $|\theta_2 - \theta_3|$ is expected so that the power stroke can take place.

2.3. Equations of motion

In addition to the force from the time-varying potential, the motor proteins are subject to frictional and random forces due to collision with other molecules in the cytosol. Assuming that the motion is overdamped, the equation

of motion is given by the Langevin equation

$$\dot{x} = -\frac{\partial V(x,\theta,t)}{\partial x} + F_{ext} + \xi_x(t) \quad (5)$$

$$\dot{\theta} = -\frac{\partial V(x,\theta,t)}{\partial \theta} + \xi_\theta(t) \quad (6)$$

where F_{ext} is an external force and the Langevin force ξ_i is defined by

$$\langle \xi_i(t)\xi_i(t')\rangle = 2D_i\delta(t-t') \qquad i \in (x,\theta) \quad (7)$$

with a diffusion constant D_i. In this paper, we assume $D_x = D_\theta = D$. The time-dependent potential $V(x,\theta,t)$ alternately takes one of the potential values V_i. We use two different switching method: one is a deterministic periodic switching and the other is a stochastic transition based on the transition rates k_{ij}. The Langevin equation is integrated using the Heun method and the average was taken over a sufficient number of realizations.

3. RESULTS

3.1. A single motor with two states

We first investigate simple cases using the two-state model. Figure 2 shows the average velocity of the motor protein as a function of the conformational change $\Delta\theta = \theta_1 - \theta_3$. The parameter values are chosen such that the powerstroke mechanism is possible only when $\Delta\theta > 0.5$. The left panel of Fig. 2 uses the periodic switching with the period of T=4. The motor spends half the period in each potential. In the absence of diffusion ($D = 0$), the only mechanism capable of providing motion is the powerstroke mechanism. In principle the motor can move for $\Delta\theta > 0.5$ provided that there is enough time to reach an equilibrium point in each potential. Since T=4 is not long enough, power stroke actually takes place at a larger conformational change. When the diffusion is activated, the motor moves even when the conformational change is smaller when the powerstroke is not possible. This movement is due to the Brownian motor mechanism.

In Fig. 2b, the stochastic switching between V_1 and V_3 is used. Although on average the transition time is equivalent to the periodic case, very slow or fast transitions can occasionally occur. The diffusionless curve show the contribution of the power stroke. When the conformation change is large ($\Delta\theta > 1.0$), the power stroke dominates. On the other hand, only the Brownian motor mechanism generates the motion for the small conformational change ($\Delta\theta < 0.5$). In between, both the power stroke and Brownian motor contributes.

While it is difficult to investigate the stochastic dynamics of two degrees of freedom in general, some useful insight can be obtained from an adiabatic limit. We assume that the motor protein spends sufficiently long time on each potential such that it reaches to the equilibrium point on each potential. When the protein is in V_1, the probability density can be expressed as

$$\begin{aligned} P(x,\theta,\tau) &= P_{rot}(\theta)P_{trans}(x,\tau) \\ &= N\exp(-\alpha x^2)\exp(-\beta\theta^2) \end{aligned} \quad (8)$$

where $P_{rot}(\theta)$ and $P_{trans}(x,\tau)$ are probability densities for Uhlenbeck and Wiener processes, respectively. In the second line of Eqn. (8), $N = \frac{1}{\sqrt{4\pi D\tau}}\sqrt{\frac{k}{2\pi D}}$, $\alpha = \frac{1}{4D\tau}$, and $\beta = \frac{k}{2D}$. Integrating the portion of P that lies over the next potential well allows us to find the probability of making a step forward.

$$W_{+1} = \int_{-\infty}^{\infty} dx \int_{-\infty}^{(x-1/2)/r} d\theta P_{rot}(\theta)P_{trans}(x,\tau) \quad (9)$$

$$= \frac{1}{2}\left[\mathrm{erf}\left(\frac{\gamma}{2r}\right) + 1\right] \quad (10)$$

where $\gamma^{-1} = \sqrt{\frac{m^2}{\alpha} + \frac{1}{\beta}}$. Figure 3a shows close agreement between the adiabatic theory and the stochastic simulation given a slow enough switching rate.

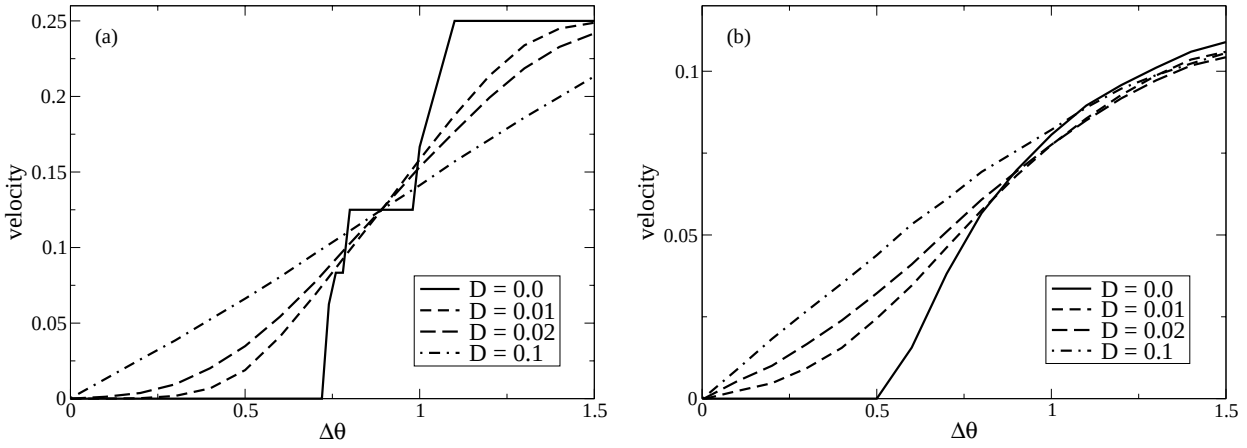

Figure 2. The velocity of the motor proteins $\langle \dot{x} \rangle$ as a function of conformational change $\Delta\theta$. Parameter values $K_1 = K_3 = 1.0$ and $U_3 = 1.0$ are used and the average was taken over 100 samples. (a) Periodic switching with the period T=4. (b) Stochastic switching with $\bar{k}_{13} = \bar{k}_{31} = 0.5$.

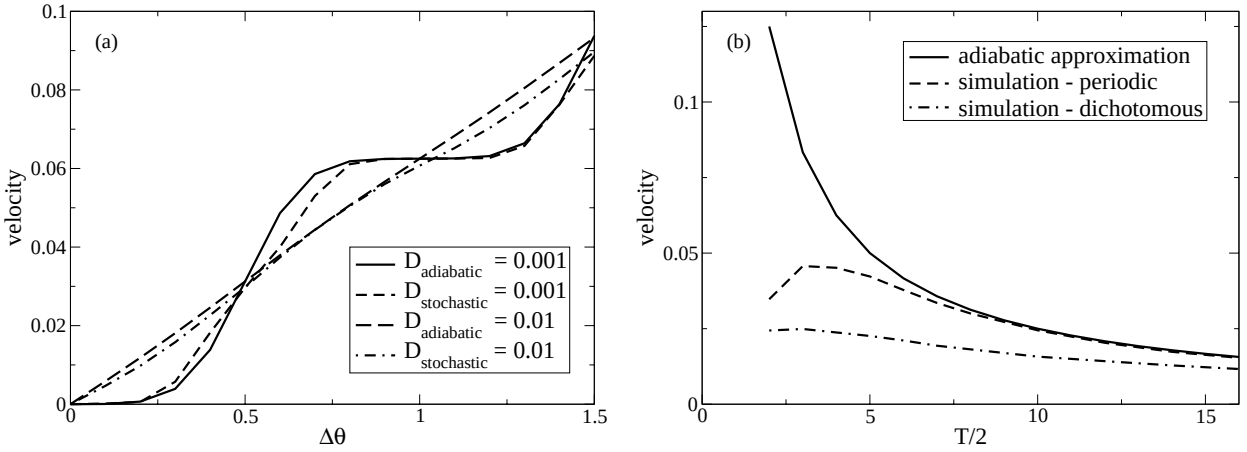

Figure 3. (a) Comparison of adiabatic theory and numerical stochastic simulations. Parameters: $\Delta\theta = 1.0$, $K_1 = K_3 = 1.0$, $U_3 = 1.0$, $T = 16$, $D = 0.01$; (b) The convergence of the adiabatic theory with stochastic simulations. Parameters: $\Delta\theta = 0.5$, $K_1 = K_3 = 1.0$, $U_3 = 1.0$, $D = 0.01$

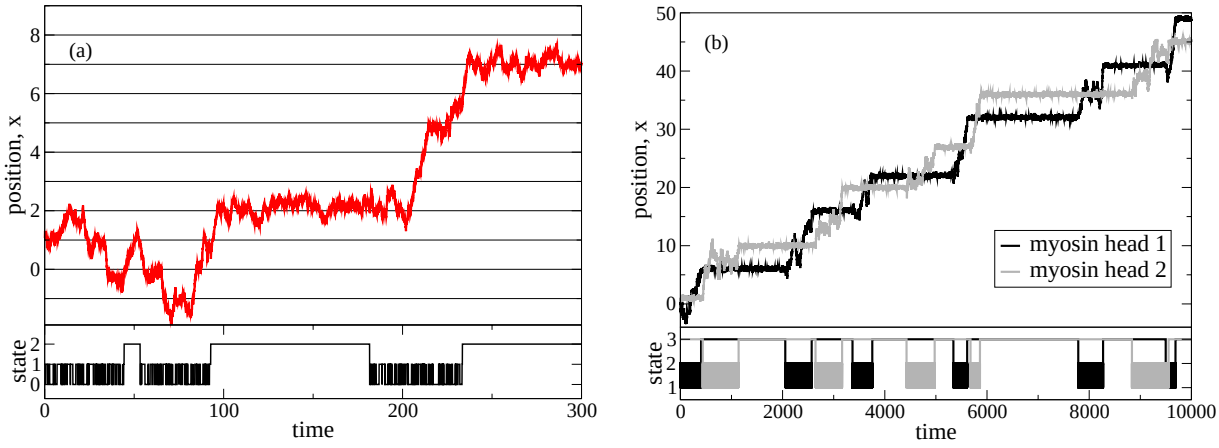

Figure 4. (a) The movement of a single myosin head driven by trichotomous switching between V_1, V_2, and V_3. (b) Dimer system of motors driven by trichotomous potentials and coupled by the force in Eqn. 15. Parameters: $U_2 = 0.5$, $U_3 = 1.0$, $\theta_1 = 0.0$, $\theta_2 = -0.2$, $\theta_3 = 1.0$, $D = 0.1$, $k_{12} = k_{21} = 2.0$, $k_{23} = 0.05$, $k_{31} = 0.01$, $k_{32} = k_{13} = 0.0$; dimer interaction — $F_0 = 0.1$, $d_0 = 5.0$, $\Delta d = 2.0$

3.2. A single motor with three states

We choose parameters for the three-state model described by Eqn. 4 such that rapid switching exists between V_1 and V_2 with a small conformational change between θ_1 and θ_2, allowing for the Brownian motor mechanism to take place. As for the third state, the system doesn't enter the state very often compared to the Brownian phase of movement, and once it does the system is frozen until another ATP nucleotide binds to the motor domain.

In Fig. 4a, we observe a remarkable similarity between the simulation data and experimental data performed on single molecules of myosin II.[25] The motor protein is observed to move steadily for several periods during the hydrolysis cycle of a single ATP nucleotide. The fact that single myosin heads move along an actin filament after hydrolyzing a single ATP molecule in multiple steps that correspond very closely to the period of actin subunits — 5.3 nm — is a phenomenon which lends support to a Brownian motor mechanism and which is replicated by the simulation results seen in Fig. 4a.

3.3. Myosin V: a pair of coupled motors

In the previous section, we investigated the motility of a single myosin head. However, myosin proteins have two motor domains attached to each bundled tail. The cooperation of each individual head is still unclear, particularly with the myosin II found in skeletal muscle. However, experiments done on the processive myosin V protein have yielded evidence that the two heads move in a coordinated way that when one is moving forward, the other is bound to the actin filament.[7, 23, 34] Such coordination has a big advantage since one of the heads is always bound to the filament and prevents backward sliding or diffusion away from the filament. However, the mechanism of this processive motion has not been determined yet.

It has been known that myosin V makes a stepwise motion with a large step length of 38 nm. Such a long step can be explained by a lever arm mechanism since myosin V has a sufficiently long lever arm. However, it is unlikely that such a big swing puts the head on the right spot on the actin filament, especially under strong thermal fluctuation. It is more natural to assume that the actin filament navigates the heads.

Our model of myosin V consists of two motors each driven by the three-state model described in the previous section. In addition, there is a coupling force between them. The equations of motion of the heads A and B are

given by

$$\dot{x}_A = -\frac{\partial V(x_A, \theta_A, t)}{\partial x_A} + F_{ext} + F_{AB} + \xi_{xA}(t) \quad (11)$$

$$\dot{x}_B = -\frac{\partial V(x_B, \theta_B, t)}{\partial x_B} + F_{ext} + F_{BA} + \xi_{xB}(t) \quad (12)$$

$$\dot{\theta}_A = -\frac{\partial V(x_A, \theta_A, t)}{\partial \theta_A} + \xi_{\theta A}(t) \quad (13)$$

$$\dot{\theta}_B = -\frac{\partial V(x_B, \theta_B, t)}{\partial \theta_B} + \xi_{\theta B}(t) \quad (14)$$

where the coupling force takes the following form:

$$F_{AB} = -F_{BA} = F_0 \sigma(|x_A - x_B|) \quad (15)$$

$$\sigma(|x_A - x_B|) = 1 + \tanh\left(\frac{|x_A - x_B| - d_0}{\Delta d}\right) \quad (16)$$

where the function $\sigma(|x_A - x_B|)$ indicates the strain in the neck of the motor. This coupling is weak when the distance between two heads are shorter than d_0 but increases rapidly when the distance reaches d_0, preventing the heads from separating from each other beyond d_0.

To make a step wise motion, there must be communication of some type between the two motors. When one motor in front binds to the actin, the other in back must be detached and start to move forward. One possible channel of communication is the mechanical strain caused by a large separation of the two heads. We assume that the transition rate k_{31} increases when the distance between the motors reaches the limit. For simplicity, we use a strain dependent transition rate $k'_{31} = k_{31}\sigma(|x_A - x_B|)$.

Figure 4b illustrates typical trajectories of a coupled dimer. Similar to the experimental observation,[7] the two motors move processively. However, the step-wise motion with the large step length is not caused by a swing of long lever arms. The motors mainly move as Brownian motors and act as an anchor when they strongly bind to the actin filament. Since the Brownian motors often weakly bind to the filament, they move along the filament.

3.4. Response to applied force

In biological systems, motor proteins do work against an external load, be it as part of a contraction in muscle fibers or pulling vesicle cargo in an intracellular environment. Fig. 5 shows the response of the model systems discussed in the previous sections to a constant force. In Fig. 5a, the single motor driven by two-states model shows a simple linear response. While it can move against external force the maximum load is rather small. This is because the single head motor is detached from the actin filament during a certain period and slides back. On the other hand, the dimer shows a distinct non-linearity. Since one of the heads is always bound to the filament, the two motors maintain their position against a larger applied force despite the fact that it is beyond the ability to continue moving forward in any fashion as shown in Fig. 5b. A similar nonlinear response is found in actual muscle-load experiments.[28]

3.5. Cooperative Motion

The protein in skeletal muscle is arranged such that the long protein tails of myosin II are bundled into the thick filament, with the individual myosin heads protruding at regular intervals along the filament. Here we are interested in the cooperative motion of the entire bundle as each motor protein interacts with the actin filament as well as the protein bundle to which it is attached. To simulate the arrangement of myosin in muscle fibers, each motor is assumed to interact with a large backbone filament through a spring. The equations of motion for

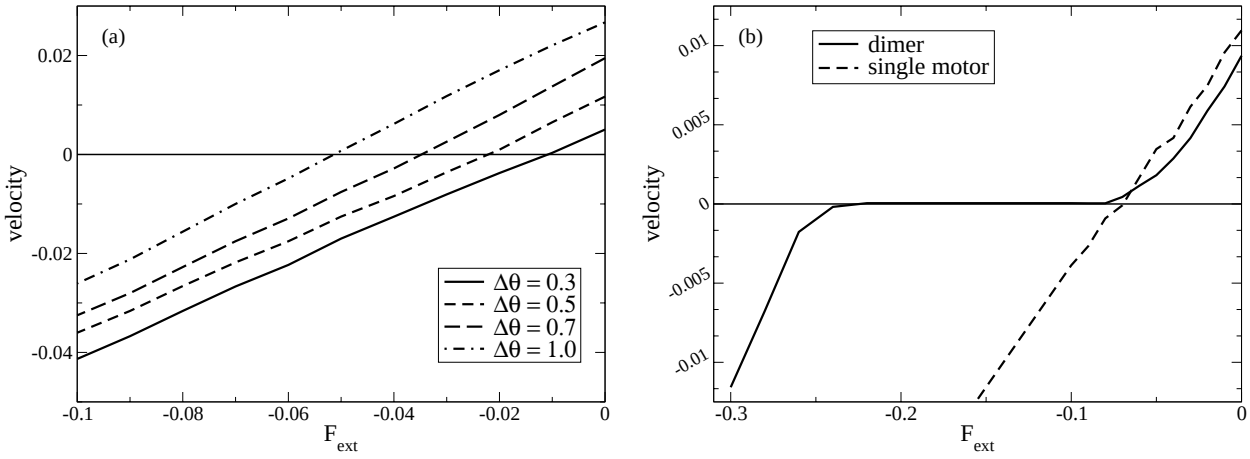

Figure 5. (a) Two state model response to externally applied force. Parameters: $K_1 = K_3 = 1.0$, $U_3 = 1.0$, $T = 16$, $D = 0.01$; (b) Three state and three state dimer response to applied force. Parameters: $U_2 = 0.5$, $U_3 = 1.0$, $\theta_1 = 0.0$, $\theta_2 = -0.2$, $\theta_3 = 1.0$, $D = 0.1$

N motors coupled to one thick filament are modeled by

$$\dot{x}_n = -\frac{\partial V(x_n, \theta_n, t)}{\partial x_n} - K_b(x_n - X_n) + \xi_{xn}(t) \tag{17}$$

$$\dot{\theta}_n = -\frac{\partial V(x_n, \theta_n, t)}{\partial \theta_n} + \xi_{\theta n}(t) \tag{18}$$

$$\dot{X} = \frac{1}{\Gamma}\left(\sum_{i=1}^{N} K_b(x_n - X_n) + F_{ext}\right) \tag{19}$$

where $X_n = X + nD(n = 1, \ldots, N)$ is a point on the thick filament where the n-th myosin is attached and D is the nearest neighbor distance between myosins. The individual motors x_n independently interact with their immediate actin filament according to the two-state model, while their interaction with the thick filament is governed by $K_b(x_n - X_n)$. The velocity of the thick filament is given by $\dot{X}(t)$ which is subject to a large drag Γ and pulled by the sum of the individual motors through the spring interactions. The effect of Γ on the sliding velocity of the filament is seen in Fig. 6a. As expected for a large number of motors, the drag on the backbone has a diminishing effect, but the maximum velocity of the filament cannot be any faster than that of the individual motors. The maximum attainable force by the filament and motors, on the other hand, increases linearly with the number of motors attached depending on the strength of the spring interaction, K_b.

4. DISCUSSION

Despite the variety of models that have been proposed since Huxley first discovered the sliding filament model of muscle contraction, underlying elements of similarity should exist between the different families of myosin. The model proposed here attempts to resolve some of those differences. Experimental evidence favors a Brownian motion model for cooperative motors such as myosin II, modeled here by the shallow change in the stable angle $\Delta\theta$ between two chemical states. Single-molecule experiments have shown that myosin can take several small steps during the hydrolysis cycle of only one ATP molecule.[25]

Experiments conducted with myosin V on the other hand have shown a great deal of evidence lending credence to the concept of a hand-over-hand model in which the individual heads of the motor work together in a cooperative manner of some sort giving rise to the processive motion. Incorporating this feature into the model

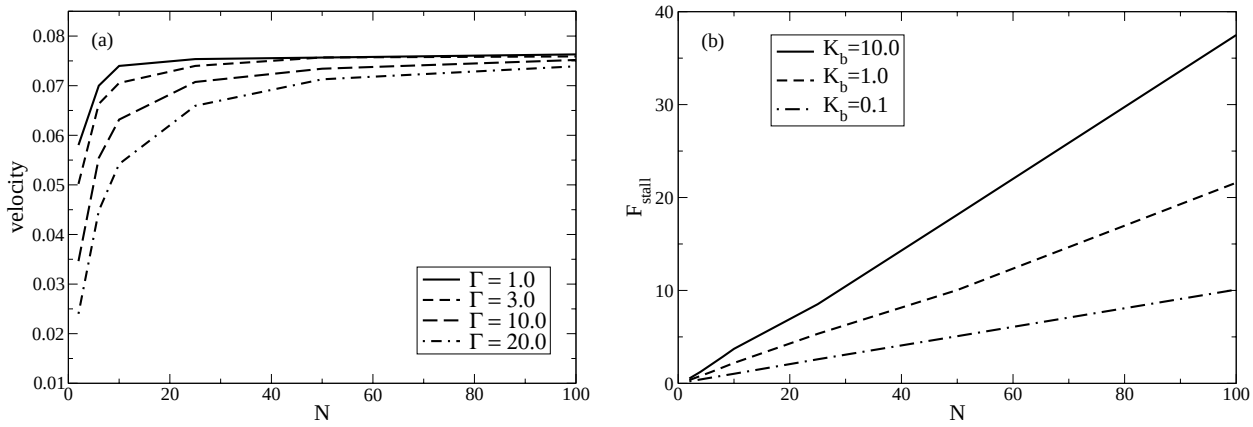

Figure 6. Cooperative motion between N motors and a single thick filament. (a) Velocity response to a fixed drag Γ on the backbone of the myosin bundle. Parameters: $K_1 = K_3 = 1.0$, $U_3 = 1.0$, $\Delta\theta = 1.0$, $k_{13} = k_{31} = 0.125$, $D = 0.01$, $K_b = 10.0$; (b) Maximum attainable force (F_{stall}) by N motors coupled by a spring to a protein bundle. Parameters: $K_1 = K_3 = 1.0$, $U_3 = 1.0$, $\Delta\theta = 1.0$, $k_{12} = k_{21} = 0.125$, $D = 0.01$, $\Gamma = 20.0$

presented here amounts to simply increasing the stable angle between states to a larger value corresponding to a deterministic stroke.

The beauty of the model presented here, is that given different parameters and definitions for the interaction between individual motor proteins, we can qualitatively reproduce many of the results already collected by researchers in both the fields of processive and non-processive motors. More experimentation remains to be done to discover the extent to which this model works.

ACKNOWLEDGMENTS

Authors B.G. and R.K. would like to thank Dr. Herbert C Cheung and Dr. John Robinson for many enlightening conversations concerning the details of muscle physiology and chemistry. This work is partially supported by National Science Foundation (NSF) Grant No. PHY-0354937, NSF GK-12 Award No. 0139108, and NSF Research Experience for Undergraduates (REU) site Grant No. DMR-0243640.

REFERENCES

1. H. E. Huxley, "Electron microscope studies of the organisation of the filaments in striated muscle," *Biohem. Biophys. Acta* **12**, pp. 387–394, 1953.
2. A. F. Huxley and R. Niedergerke, "Interference microscopy of living muscle fibres," *Nature* **173**, pp. 971–973, 1954.
3. A. F. Huxley, "Muscle structure and theories of contraction," *Prog. Biophys. Biophys. Chem.* **7**, pp. 255–318, 1957.
4. A. F. Huxley and R. M. Simmons, "Proposed mechanism of force generation in striated muscle," *Nature* **233**, pp. 533–538, 1971.
5. R. Cooke, "The sliding fillament model: 1972–2004," *J. Gen. Physiol.* **123**, pp. 643–656, June 2004. (*See also references therein*)
6. A. F. Huxley, "Mechanics and models of the myosin motor," *Phil. Trans. R. Soc. Lond. B* **355**, pp. 433–440, 2000. (*See also references therein*)
7. J. N. Forkey, M. E. Quinlan, M. A. Shaw, *et al.*, "Three-dimensional structural dynamics of myosin V by single-molecule fluorescence polarization," *Nature* **422**, pp. 399–403, 2003.

8. I. Rayment, W. R. Rypniewski, K. Schmidt-Base, *et al.*, "Three-dimensional structure of myosin subfragment-1: A molecular motor," *Science* **261**, pp. 50–58, July 1993.
9. M. Whittaker, E. M. Wilson-Kubalek, J. E. Smith, *et al.*, "A 35-Å movement of smooth muscle myosin on ADP release," *Nature* **378**, pp. 748–751, 1995.
10. J. D. Jontes, E. M. Wilson-Kubalek, and R. A. Milligan, "A 32° tail swing in brush border myosin I on ADP release," *Nature* **378**, pp. 751–753, 1995.
11. A. Houdusse, A. G. Szent-Gyorgyi, and C. Cohen, "Three conformational states of scallop myosin S1," *PNAS* **97**(21), pp. 11238–11243, 2000.
12. M. Anson, M. A. Geeves, S. E. Kurzawa, *et al.*, "Myosin motors with artificial lever arms," *EMBO J.* **15**(22), pp. 6069–6074, 1996.
13. T. Q. P. Uyeda, P. D. Abramson, and J. A. Spudich, "The neck region of the myosin motor domain acts as a lever arm to generate movement," *PNAS* **93**, pp. 4459–4464, April 1996.
14. T. Sakamoto, F. Wang, S. Schmitz, *et al.*, "Neck length and processivity of myosin V," *J. Bio. Chem.* **278**(31), pp. 29201–29207, 2003.
15. T. J. Purcell, C. Morris, J. A. Spudich, *et al.*, "Role of the lever arm in the processive stepping of myosin V," *PNAS* **99**(22), pp. 14159–14164, 2002.
16. D. H. Schott, R. N. Collins, and A. Bretscher, "Secretory vesicle transport velocity in living cells depends on the myosin-V lever arm length," *J. Cell. Biol.* **156**(1), pp. 35–39, 2002.
17. C. Ruff, M. Furch, B. Brenner, *et al.*, "Single-molecule tracking of myosins with genetically engineered amplifier domains," *Nat. Struc. Biol.* **8**(3), pp. 226–229, 2001.
18. D. M. Warshaw, W. H. Guilford, Y. Freyzon, *et al.*, "The light chain binding domain of expressed smooth muscle heavy meromyosin acts as a mechanical lever," *J. Biol. Chem.* **275**(47), pp. 37167–37172, 2000.
19. S. Itakura, H. Yamakawa, Y. Y. Toyoshima, *et al.*, "Force-generating domain of myosin motor," *Biochem. Biophys. Res. Commun.* **196**(3), pp. 1504–1510, 1993.
20. K. M. Trybus, E. Krementsova, and Y. Freyzon, "Kinetic characterization of a monomeric unconventional myosin V construct," *J. Biol. Chem.* **274**(39), pp. 27448–27456, 1999.
21. C. Perreault-Micale, A. D. Shushan, and L. M. Coluccio, "Truncation of a mammalian myosin I results in loss of Ca2+-sensitive motility," *J. Biol. Chem.* **275**(28), pp. 21618–21623, 2000.
22. K. Homma, J. Saito, R. Ikebe, *et al.*, "Ca2+-dependent regulation of the motor activity of myosin V," *J. Biol. Chem.* **275**(44), pp. 34766–34771, 2000.
23. H. Tanaka, K. Homma, A. H. Iwane, *et al.*, "The motor domain determines the large step of myosin-V," *Nature* **415**, pp. 192–95, 2002.
24. I. Lister, S. Schmitz, M. Walker, *et al.*, "A monomeric myosin VI with a large working stroke," *EMBO J.* **23**(8), pp. 1729–1738, 2004.
25. K. Kitamura, M. Tokunaga, A. H. Iwane, *et al.*, "A single myosin head moves along an actin filament with regular steps of 5.3 nanometres," *Nature* **397**, pp. 129–134, 1999.
26. J. Howard, *Mechanics of Motor Proteins and the Cytoskeleton*, Sinauer Associates, Inc., Sunderland, MA, 2001.
27. A. Ishijima, H. Kojima, T. Funatsu, *et al.*, "Simultaneous observation of individual ATPase and mechanical events by a single myosin molecule during interaction with actin," *Cell* **92**, pp. 161–71, 1998.
28. J. Keener and J. Sneyd, *Mathematical Physiology*, Springer-Verlag, New York, 1998.
29. D. Keller and C. Bustamante, "The mechanochemistry of molecular motors," *Biophys. J.* **78**, pp. 541–556, 2000.
30. C. Veigel, L. M. Coluccio, J. D. Jontes, *et al.*, "The motor protein myosin-I produces its working stroke in two steps," *Nature* **398**, pp. 530–33, 1999.
31. P. Reimann, "Brownian motors: noisy transport far from equilibrium," *Phys. Rep.* **361**, pp. 57–265, 2002. (*See also references therein*)
32. R. D. Astumian, "Making molecules into motors," *Sci. Am.* **285**, pp. 56–64, July 2001.
33. R. D. Astumian and P. Hänggi, "Brownian motors," *Physics Today* **55**, pp. 33–39, Nov 2002.
34. A. Yildiz, J. N. Forkey, S. A. McKinney, *et al.*, "Myosin V walks hand-over-hand: Single fluorophore imaging with 1.5-nm localization," *Science* **300**, pp. 2061–2065, 2003.